Inorg. Chem. **2003**, *42*, 8395–8405

Substituent Effects of β-Diketiminate Ligands on the Structure and Physicochemical Properties of Copper(II) Complexes

Chizu Shimokawa,[†] Seiji Yokota,[†] Yoshimitsu Tachi,[†] Nagatoshi Nishiwaki,[‡] Masahiro Ariga,[‡] and Shinobu Itoh*,[†]

Department of Chemistry, Graduate School of Science, Osaka City University, 3-3-138 Sugimoto, Sumiyoshi-ku, Osaka 558-8585, Japan, and Department of Chemistry, Osaka Kyoiku University, 4-698-1 Asahigaoka, Kashiwara, Osaka 582-8582, Japan

Received May 7, 2003

Substituent effects of β-diketiminate ligands on the structure and physicochemical properties of the copper(II) complexes have been systematically investigated by using 3-iminopropenylamine derivatives $^{R1}L^{R3}H$, R^3—N═CH—C(R^1)═CH—NH—R^3, where R^1 is Me, H, CN, or NO_2, and R^3 is Ph, Mes (mesityl), Dep (2,6-diethylphenyl), Dipp (2,6-diisopropylphenyl), or Dtbp (3,5-di-*tert*-butylphenyl). When the ligands with R^3 = Ph or Dtbp were treated with $Cu^{II}(OAc)_2$, bis(β-diketiminate) copper(II) complexes exhibiting distorted tetrahedral geometries were obtained, the crystal structures of which were nearly the same as each other regardless of the α-substituent (R^1); dihedral angles between the two β-diketiminate coordination planes are 62.5 ± 1.2°, and the Cu–N bond lengths are 1.959 ± 0.008 Å. The distorted tetrahedral structures are maintained in solution, but the spectroscopic features, especially $g_{||}$ values of the ESR spectra and the d–d bands of the absorption spectra, as well as the electrochemical behaviors of the complexes, are significantly affected by the electronic nature of R^1. The ligands with R^3 = Mes and Dep, on the other hand, gave di(μ-hydroxo)dicopper(II) complexes, and their crystal structures as well as spectroscopic and electrochemical features have also been explored. Furthermore, the ligand with the more sterically encumbered aromatic substituent (Dipp) provided a mononuclear four-coordinate square planar copper(II) complex supported by one β-diketiminate ligand and one didentate acetate ion. Thus, the β-diketiminate ligands with a variety of substituents (R^1 and R^3) have been explored to provide coordinatively unsaturated (four-coordinate) mononuclear and dinuclear copper(II) complexes with significantly different coordination geometry and properties.

Introduction

β-Diketiminate derivatives function as monoanionic didentate ligands (Chart 1), which have been applied to the synthesis of a wide variety of transition metal, main group element, and lanthanide complexes.[1] Particular attention has recently been focused on the roles of β-diketiminate complexes as polymerization catalysts, novel organometallic compounds, and active site models for metalloenzymes.[1] In these studies, sterically encumbered β-diketiminate ligands with a bulky aromatic *N*-substituent (R^3 in Chart 1) such as 2,6-diisopropylphenyl (Dipp) have been employed in order to make the complexes as mononuclear and/or coordinatively unsaturated.[1] However, the substituent pattern of the ligand framework is rather limited to R^1 = H and R^2 = Me, since most of the ligands are prepared by the condensation reaction between commercially available acetylacetone (acac) and aniline derivatives.[2]

Chart 1

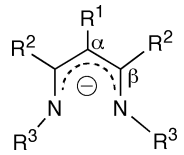

In order to control the coordination chemistry as well as the reactivity of β-diketiminate complexes, many recent efforts have been focused on the substituent effects of the carbon framework.[3−5] The bulky alkyl substituent such as *tert*-butyl group at the β-position (R^2 in Chart 1) has been shown to exhibit steric effects on the conformation of aromatic substituents R^3 (torsion angle between the aromatic

* Corresponding author. E-mail: shinobu@sci.osaka-cu.ac.jp.
† Osaka City University.
‡ Osaka Kyoiku University.

(1) Bourget-Merle, L.; Lappert, M. F.; Severn, J. R. *Chem. Rev.* **2002**, *102*, 3031−3065.

10.1021/ic0344766 CCC: $25.00
Published on Web 11/14/2003

ring of R^3 and the coordination plane of the β-diketiminate ligand) and on the bite angle of the didentate ligands. Those steric factors have been shown to induce significant effects on the structure and reactivity of the β-diketiminate complexes.[3] On the other hand, Coates and co-workers have recently demonstrated that introduction of electron-withdrawing substituents such as $-$CN and $-CF_3$ into the carbon framework improves the catalytic efficiency of the zinc(II) complexes in the CO_2/epoxide copolymerization reaction and the ring opening polymerization of β-lactones.[4] Furthermore, a nitro group at the α-position (R^1) has been demonstrated to act as a bridging ligand to construct a novel linear polymer complex of copper(I).[5] Thus, further ligand modifications may have great potential in expanding the chemistry of β-diketiminate complexes. However, systematic studies on the substituent effects both of the ligand framework and of the *N*-aryl group have yet to be reported.

In this study, a series of β-diketiminate ligands carrying a different α-substituent (R^1 = Me, H, CN, and NO_2) have been employed for the synthesis of copper(II) complexes in order to get insights into the electronic effects of R^1 on the structures and physicochemical properties of the complexes. Moreover, steric effects of the *N*-aryl groups have also been examined using different aromatic groups (R^3 = Ph, Mes, Dep, Dipp, Dtbp, see Chart 2) to demonstrate that the *N*-aryl group significantly influences the structure of the resulting copper(II) complexes.

Chart 2

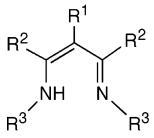

$^{R1}L^{R3}H$	R^1	R^3
$^{Me}L^{Ph}H$	Me	phenyl
$^{H}L^{Ph}H$	H	phenyl
$^{CN}L^{Ph}H$	CN	phenyl
$^{CN}L^{Mes}H$	CN	mesityl
$^{CN}L^{Dep}H$	CN	2,6-diethylphenyl
$^{CN}L^{Dipp}H$	CN	2,6-diisopropylphenyl
$^{NO_2}L^{Ph}H$	NO_2	phenyl
$^{NO_2}L^{Mes}H$	NO_2	mesityl
$^{NO_2}L^{Dtbp}H$	NO_2	3,5-di-*tert*-butylphenyl

R^2 = H

Experimental Section

General. Reagents and solvents used in this study except the ligands and the complexes were commercial products of the highest available purity and were further purified by the standard methods, if necessary.[6] Ligands $^{Me}L^{Ph}H$ and $^{H}L^{Ph}H$ and their copper(II) complexes were prepared according to the reported procedures.[7,8] 1-Methyl-5-nitro-1*H*-pyrimidin-2-one (**1**) was prepared according to the reported methods.[9] FT-IR spectra were recorded with a Shimadzu FTIR-8200PC. Mass spectra were recorded with a JEOL JMS-700T Tandem MS station. ^{1}H NMR spectra were recorded on a JEOL LMN-ECP300WB or a LMX-GX400. ESR measurements were performed of frozen THF solutions on the copper(II) complexes using a JEOL JES-ME spectrometer at -150 °C equipped with a variable temperature cell holder. Electronic spectra were measured using a Hewlett-Packard HP8453 diode array spectrophotometer or a Hitachi U-3500L spectrophotometer. The λ_{max} and ϵ values were determined by spectral resolution with Gaussian functions using Igor Pro software (version 4, Hulinks). Elemental analyses were recorded with a Perkin-Elmer or a Fisons instruments EA1108 Elemental Analyzer.

X-ray Structure Determination. The single crystal was mounted on a glass-fiber. X-ray diffraction data were collected by a Rigaku RAXIS-RAPID imaging plate two-dimensional area detector using graphite-monochromated Mo Kα radiation (λ = 0.71069 Å) to $2\theta_{max}$ of 55.0°. All the crystallographic calculations were performed using Crystal Structure software package of the Molecular Structure Corporation (version 2.0 and 3.1). The crystal structures were solved by the direct methods and refined by the full-matrix least-squares using SIR-92 or SHELX97. All non-hydrogen atoms and hydrogen atoms were refined anisotropically and isotropically, respectively.

(2) Some of the recent works dealing with β-diketiminate ligands derived from acac (R^1 = H, R^2 = Me in Chart 1): (a) Holland, P. L.; Tolman, W. B. *J. Am. Chem. Soc.* **2000**, *122*, 6331−6332. (b) Cheng, M.; Moore, D. R.; Reczek, J. J.; Chamberlain, B. M.; Lobkovsky, E. B.; Coates, G. W. *J. Am. Chem. Soc.* **2001**, *123*, 8738−8749. (c) Panda, A.; Stender, M.; Wright, R. J.; Olmstead, M. M.; Klavins, P.; Power, P. P. *Inorg. Chem.* **2002**, *41*, 3909−3916. (d) Eckert, N. A.; Bones, E. M.; Lachicotte, R. J.; Holland, P. L. *Inorg. Chem.* **2003**, *42*, 1720−1725. (e) Fekl, U.; Goldberg, K. I. *J. Am. Chem. Soc.* **2002**, *124*, 6804−6805. (f) Stender, M.; Wright, R. J.; Eichler, B. E.; Prust, J.; Olmstead, M. M.; Roesky, H. W.; Power, P. P. *J. Chem. Soc., Dalton Trans.* **2001**, 3465−3469. (g) Jancik, V.; Peng, Y.; Roesky, H. W.; Li, J.; Neculai, D.; Neculai, A. M.; Herbst-Irmer, R. *J. Am. Chem. Soc.* **2003**, *125*, 1452−1453. (h) Gibson, V. C.; Segal, J. A.; White, A. J. P.; Williams, D. J. *J. Am. Chem. Soc.* **2000**, *122*, 7120−7121. (i) Stender, M.; Eichler, B. E.; Hardman, N. J.; Power, P. P.; Prust, J.; Noltemeyer, M.; Roesky, H. W. *Inorg. Chem.* **2001**, *40*, 2794−2799. (j) Willems, S. T. H.; Budzelaar, P. H. M.; Moonen, N. N. P.; de Gelder, R.; Smits, J. M. M.; Gal, A. W. *Chem. Eur. J.* **2002**, *8*, 1310−1320. (k) MacAdams, L. A.; Kim, W.-K.; Liable-Sands, L. M.; Guzei, I. A.; Rheingold, A. L.; Theopold, K. H. *Organometallics* **2002**, *21*, 952−960. (l) Ding, Y.; Ma, Q.; Usón, I.; Roesky, H. W.; Noltemeyer, M.; Schmidt, H.-G. *J. Am. Chem. Soc.* **2002**, *124*, 8542−8543. (m) Yao, Y.; Zhang, Y.; Shen, Q.; Yu, K. *Organometallics* **2002**, *21*, 819−824. (n) Burford, N.; Ragogna, P. J.; Robertson, K. N.; Cameron, T. S.; Hardman, N. J.; Power, P. P. *J. Am. Chem. Soc.* **2002**, *124*, 382−383. (o) Cui, C.; Kölpke, S.; Herbst-Irmer, R.; Roesky, H. W.; Noltemeyer, M.; Schmidt, H.-G.; Wrackmeyer, B. *J. Am. Chem. Soc.* **2001**, *123*, 9091−9098.

(3) (a) Budzelaar, P. H. M.; van Oort, A. B.; Orpen, A. G. *Eur. J. Inorg. Chem.* **1998**, 1485−1494. (b) Jazdzewski, B. A.; Holland, P. L.; Pink, M.; Young, V. G., Jr.; Spencer, D. J. E.; Tolman, W. B. *Inorg. Chem.* **2001**, *40*, 6097−6107. (c) Spencer, D. J. E.; Aboelella, N. W.; Reynolds, A. M.; Holland, P. L.; Tolman, W. B. *J. Am. Chem. Soc.* **2002**, *124*, 2108−2109. (d) Aboelella, N. W.; Lewis, E. A.; Reynolds, A. M.; Brennessel, W. W.; Cramer, C. J.; Tolman, W. B. *J. Am. Chem. Soc.* **2002**, *124*, 10660−10661. (e) Spencer, D. J. E.; Reynolds, A. M.; Holland, P. L.; Jazdzewski, B. A.; Duboc-Toia, C.; Le Pape, L.; Yokota, S.; Tachi, Y.; Itoh, S.; Tolman, W. B. *Inorg. Chem.* **2002**, *41*, 6307−6321. (f) Smith, J. M.; Lachicotte, R. J.; Holland, P. L. *Chem. Commun.* **2001**, 1542−1543. (g) Smith, J. M.; Lachicotte, R. J.; Pittard, K. A.; Cundari, T. R.; Lukat-Rodgers, G.; Rodgers, K. R.; Holland, P. L. *J. Am. Chem. Soc.* **2001**, *123*, 9222−9223. (h) Bailey, P. J.; Coxall, R. A.; Dick, C. M.; Fabre, S.; Parsons, S. *Organometallics* **2001**, *20*, 798−801. (i) Caro, C. F.; Hitchcock, P. B.; Lappert, M. F. *Chem. Commun.* **1999**, 1433−1434. (j) Hayes, P. G.; Piers, W. E.; Lee, L. W. M.; Knight, L. K.; Parvez, M.; Elsegood, M. R. J.; Clegg, W. *Organometallics* **2001**, *20*, 2533−2544. (k) Hayes, P. G.; Piers, W. E.; McDonald, R. *J. Am. Chem. Soc.* **2002**, *124*, 2132−2133.

(4) (a) Allen, S. D.; Moore, D. R.; Lobkovsky, E. B.; Coates, G. W. *J. Am. Chem. Soc.* **2002**, *124*, 14284−14285. (b) Moore, D. R.; Cheng, M.; Lobkovsky, E. B.; Coates, G. W. *Angew. Chem., Int. Ed.* **2002**, *41*, 2599−2602.

(5) Yokota, S.; Tachi, Y.; Nishiwaki, N.; Ariga, M.; Itoh, S. *Inorg. Chem.* **2001**, *40*, 5316−5317.

(6) Perrin, D. D.; Armarego, W. L. F.; Perrin, D. R. *Purification of Laboratory Chemicals*, 4th ed.; Pergamon Press: Elmsford, NY, 1996.

(7) Klimko, V. T.; Skoldinov, A. P. *Zh. Obshch. Khim.* **1959**, *29*, 4027−4029.

(8) Tsybina, N. M.; Vinokurov, V. G.; Protopopova, T. V.; Skoldinov, A. P. *J. Gen. Chem. USSR* **1966**, *36*, 1383−1385.

(9) Nishiwaki, N.; Tohda, Y.; Ariga, M. *Bull. Chem. Soc. Jpn.* **1996**, *69*, 1997−2002.

Atomic coordinates, thermal parameters, and intramolecular bond distances and angles are deposited in the Supporting Information as in CIF file format.

Electrochemical Measurement. The cyclic voltammetry was performed on an ALS electrochemical analyzer CHI-630A in deaerated THF containing 0.10 M n-Bu_4NClO_4 as supporting electrolyte. The Pt electrode was polished with BAS polishing alumina suspension, rinsed with THF, and dried before use. The counter electrode was a platinum wire. The measured potentials were recorded with respect to a Fc/Fc^+ (2.0×10^{-3} M) reference electrode. All electrochemical measurements were carried out under an atmospheric pressure of Ar in a glovebox.

Theoretical Calculations. The heat of formation (ΔH_f) values of $^{NO_2}L^{Ar}H$ were calculated using the PM3 semiempirical molecular orbital method.[10] The calculations were performed using the CAChe program version 3.2. Final geometries and energetics were obtained by optimizing the total molecular energy with respect to all structural variables.

Synthesis. 2-Cyano-*N*-phenyl-3-phenylamino-2-propeneimine ($^{CN}L^{Ph}H$). This compound was prepared by the reported method by Noguchi and co-workers as follows.[11] To a solution of 1,3,3-tributoxy-2-cyanopropene (50.1 wt % in butanol, 10 mL, 15 mmol) was added water (10 mL) and concentrated hydrochloric acid (5 mL), and the mixture was stirred at room temperature for 48 h. The reaction mixture was extracted with methylene chloride (50 mL × 3), and the combined organic layer was dried over anhydrous $MgSO_4$. Removal of the solvent by evaporation gave an orange liquid, to which a methanol solution (30 mL) of aniline (2.79 g, 30 mmol) was added. After refluxing the mixture for 24 h, removal of the volatile organic material under reduced pressure gave a brown oily material, from which $^{CN}L^{Ph}H$ was isolated in a 29% yield by SiO_2 column chromatography by using chloroform as an eluent. IR (KBr): 3080 (NH), 2208 (C≡N), 1641 (C═N) cm^{-1}. ^1H NMR ($CDCl_3$, 300 MHz): δ 7.15 (d, 4 H, $J = 7.5$ Hz, aromatic *o*-proton of Ph), 7.22 (t, 2 H, $J = 7.5$ Hz, aromatic *p*-proton of Ph), 7.40 (t, 4 H, $J = 7.5$ Hz, aromatic *m*-proton of Ph), 8.07 (s, 2 H, C*H*), 13.20 (br, 1 H, N*H*). HRMS (EI^+): *m*/*z* 247.1100, calcd for $C_{16}H_{13}N_3$ 247.1109. Anal. Calcd for $C_{16}H_{13}N_3$: C, 77.35; H, 5.21; N, 16.88. Found: C, 77.71; H, 5.30; N, 16.99.

2-Cyano-*N*-mesityl-3-mesitylamino-2-propeneimine ($^{CN}L^{Mes}H$). This compound was prepared in a similar manner described for the synthesis of $^{CN}L^{Ph}H$ by using 2,4,6-trimethylaniline instead of aniline in a 47% isolated yield. In this case, the reaction of 2,4,6-trimethylaniline was carried out for 48 h. Single crystals suitable for X-ray crystallographic analysis were obtained by slow diffusion of liquid methanol into a chloroform solution containing $^{CN}L^{Mes}H$. IR (KBr): 3070 (NH), 2202 (C≡N), 1644 (C═N) cm^{-1}. ^1H NMR ($CDCl_3$, 400 MHz): δ 2.19 (s, 12 H, CH_3), 2.28 (s, 6 H, CH_3), 6.90 (s, 4 H, aromatic H of mesityl group), 7.67 (s, 2 H, C*H*), 12.38 (br, 1 H, N*H*). HRMS (EI^+): *m*/*z* 331.2046, calcd for $C_{22}H_{25}N_3$ 331.2048. Anal. Calcd for $C_{22}H_{25}N_3$: C, 79.72; H, 7.60; N, 12.68. Found: C, 79.66; H, 7.67; N, 12.65.

2-Cyano-*N*-(2,6-diethylphenyl)-3-(2,6-diethylphenyl)amino-2-propeneimine ($^{CN}L^{Dep}H$). This compound was prepared in a similar manner described for the synthesis of $^{CN}L^{Ph}H$ by using 2,6-diethylaniline instead of aniline in a 35% isolated yield. In this case, the reaction of 2,6-diethylaniline was carried out for 48 h. Single crystals suitable for X-ray crystallographic analysis were obtained by slow diffusion of liquid methanol into a chloroform solution containing $^{CN}L^{Dep}H$. IR (KBr): 3110 (NH), 2201 (C≡N), 1638 (C═N) cm^{-1}. ^1H NMR ($CDCl_3$, 400 MHz): δ 1.17 (t, 12 H, $J = 7.6$ Hz, CH_3), 2.59 (q, 8 H, $J = 7.6$ Hz, CH_2), 7.10−7.16 (m, 6 H, aromatic H of Ar group), 7.69 (s, 2 H, C*H*), 12.40 (br, 1 H, N*H*). HRMS (EI^+): *m*/*z* 359.2376, calcd for $C_{24}H_{29}N_3$ 359.2361. Anal. Calcd for $C_{24}H_{29}N_3$: C, 80.18; H, 8.13; N, 11.69. Found: C, 80.01; H, 8.14; N, 11.67.

2-Cyano-*N*-(2,6-diisopropylphenyl)-3-(2,6-diisopropylphenyl)-amino-2-propeneimine ($^{CN}L^{Dipp}H$). This compound was prepared in a similar manner described for the synthesis of $^{CN}L^{Ph}H$ by using 2,6-diisopropylaniline instead of aniline in a 29% isolated yield. In this case, the reaction of 2,6-diisopropylaniline was carried out for 96 h. IR (KBr): 3190 (NH), 2210 (C≡N), 1647 (C═N) cm^{-1}. ^1H NMR ($CDCl_3$, 400 MHz): δ 1.20 (d, 24 H, $J = 6.8$ Hz, CH_3), 3.07 (septet, 4 H, $J = 6.8$ Hz, C*H*), 7.16−7.24 (m, 6 H, aromatic H of Ar group), 7.66 (s, 2 H, C*H*), 12.47 (br, 1 H, N*H*). HRMS (EI^+): *m*/*z* 415.2966, calcd for $C_{28}H_{37}N_3$ 415.2987. Anal. Calcd for $C_{28}H_{37}N_3$: C, 80.92; H, 8.97; N, 10.11. Found: C, 80.80; H, 8.94; N, 10.12.

2-Nitro-*N*-phenyl-3-phenylamino-2-propeneimine ($^{NO_2}L^{Ph}H$). Aniline (2.33 g, 25 mmol) was added into a methanol solution (150 mL) of 1-methyl-5-nitro-1*H*-pyrimidin-2-one (**1**) (1.86 g, 12 mmol). The mixture was refluxed for 24 h. After the reaction, evaporation of the solvent gave a brown oily material, from which $^{NO_2}L^{Ph}H$ was isolated in a 52% yield by flash SiO_2 column chromatography with chloroform as an eluent. IR (KBr): 3080 (NH), 1645 (C═N), 1565, 1317, 1282 (NO_2) cm^{-1}. ^1H NMR ($CDCl_3$, 300 MHz): δ 7.23−7.30 (m, 6H, aromatic proton of Ph), 7.45 (t, 4H, $J = 8.0$ Hz, aromatic *m*-proton of Ph), 9.15 (s, 2H, C*H*), 13.64 (br, 1H, N*H*). HR-MS (EI^+): *m*/*z* 267.0990, calcd for $C_{15}H_{13}N_3O_2$ 267.1008. Anal. Calcd for $C_{15}H_{13}N_3O_2$: C, 67.41; H, 4.90; N, 15.72. Found: C, 67.24; H, 4.84; N, 15.67.

***N*-Mesityl-3-mesitylamino-2-nitro-2-propeneimine ($^{NO_2}L^{Mes}H$).** 2,4,6-Trimethylaniline (850 mg, 6.3 mmol) was treated with compound **1** (510 mg, 3.3 mmol) in refluxing methanol (40 mL) for 4 days. Removal of volatile organic materials under reduced pressure gave a brown oily material, from which $^{NO_2}L^{Mes}H$ was isolated in a 27% yield by SiO_2 column chromatography with chloroform as an eluent. Single crystals suitable for X-ray crystallographic analysis were obtained by slow diffusion of liquid methanol into a chloroform solution containing $^{NO_2}L^{Mes}H$. IR (KBr): 3100 (NH), 1640 (C═N), 1574, 1305, 1291, 1272 (NO_2) cm^{-1}. ^1H NMR ($CDCl_3$, 300 MHz): δ 2.22 (s, 12H, CH_3), 2.29 (s, 6H, CH_3), 6.93 (s, 4H, aromatic H of Ar group), 8.75 (s, 2H, C*H*), 12.77 (br, 1H, N*H*). HRMS (EI^+): *m*/*z* 351.1957, calcd for $C_{21}H_{25}N_3O_2$ 351.1947. Anal. Calcd for $C_{21}H_{25}N_3O_2$: C, 71.77; H, 7.17; N, 11.96. Found: C, 71.79; H, 7.21; N, 11.75.

***N*-(3,5-Di-*tert*-butylphenyl)-3-(3,5-di-*tert*-butylphenyl)amino-2-nitro-2-propeneimine ($^{NO_2}L^{Dtbp}H$).** 3,5-Di-*tert*-butylaniline (821 mg, 4.0 mmol) in methanol (20 mL) was added to a methanol solution (20 mL) of **1** (310 mg, 2.0 mmol), and the solution was refluxed for 2 days. The resulting precipitates were collected by filtration to give $^{NO_2}L^{Dtbp}H$ in 45% yield. Single crystals suitable for X-ray crystallographic analysis were obtained by slow diffusion of liquid methanol into a CH_2Cl_2 solution containing $^{NO_2}L^{Dtbp}H$. IR (KBr): 3100 (NH), 1648 (C═N), 1564, 1295, 1274 (NO_2) cm^{-1}. ^1H NMR ($CDCl_3$, 300 MHz): δ 1.36 (s, 36H, CH_3), 7.09 (s, 4H, aromatic H of Ar group), 7.35 (s, 2H, aromatic H of Ar group), 9.15 (s, 2H, C*H*), 13.92 (br, 1H, N*H*). HRMS (EI^+): *m*/*z* 491.3504, calcd for $C_{31}H_{45}N_3O_2$ 491.3512. Anal. Calcd for $C_{31}H_{45}N_3O_2$: C, 75.72; H, 9.22; N, 8.55. Found: C, 75.48; H, 9.27; N, 8.60.

[$Cu^{II}(^{CN}L^{Ph})_2$]. Ligand $^{CN}L^{Ph}H$ (49.5 mg, 0.2 mmol) in methanol (10 mL) was added into a methanol solution (10 mL) of

(10) Stewart, J. J. P. *J. Comput. Chem.* **1989**, *10*, 209, 221−264.
(11) Takamura, S.; Yoshimiya, T.; Kameyama, S.; Nishida, A.; Yamamoto, H.; Noguchi, M. *Synthesis* **2000**, *5*, 637−639.

$Cu^{II}(OAc)_2 \cdot H_2O$ (20.0 mg, 0.1 mmol), and the mixture was stirred for 1 h at room temperature. The resulting precipitates were collected by filtration and dried to obtain green powder in 94% yield. Single crystals suitable for X-ray crystallographic analysis were obtained by slow diffusion of liquid methanol into a chloroform solution containing the complex. IR (KBr): 2205 (C≡N), 1605 (C═N) cm^{-1}. HRMS (FAB^+): *m*/*z* 556.1440, calcd for $C_{32}H_{25}CuN_6$ 556.1436. Anal. Calcd for $C_{32}H_{24}CuN_6$: C, 69.11; H, 4.35; N, 15.11. Found: C, 69.07; H, 4.27; N, 14.98.

$[Cu^{II}_2(^{CN}L^{Mes})_2(\mu\text{-}OH)_2]$. Ligand $^{CN}L^{Mes}H$ (33.1 mg, 0.1 mmol) in methanol (10 mL) was added into a methanol solution (10 mL) of $Cu^{II}(OAc)_2 \cdot H_2O$ (20.0 mg, 0.1 mmol). After addition of triethylamine (0.1 mmol), the mixture was refluxed for 48 h. The resulting precipitates were collected by filtration and dried to obtain brown powder in 73% yield. Single crystals suitable for X-ray crystallographic analysis were obtained by vapor diffusion of ether into a CH_2Cl_2 solution of the complex. IR (KBr): 3650 (μ-OH), 2203 (C≡N), 1616 (C═N) cm^{-1}. HRMS (FAB^+): *m*/*z* 803.2558, calcd for $C_{44}H_{49}Cu_2N_6O$ ($[(Cu^{II}L)_2(\mu\text{-}OH)]^+$) 803.2559. Anal. Calcd for $C_{44}H_{50}Cu_2N_6O_2$: C, 64.29; H, 6.13; N, 10.22. Found: C, 64.26; H, 6.13; N, 10.15.

$[Cu^{II}_2(^{CN}L^{Dep})_2(\mu\text{-}OH)_2]$. This compound was prepared in a similar manner described for the synthesis of $[Cu^{II}_2(^{CN}L^{Mes})_2(\mu\text{-}OH)_2]$ as brown powder in 73%. Single crystals suitable for X-ray crystallographic analysis were also obtained by vapor diffusion of ether into a CH_2Cl_2 solution of the complex. IR (KBr): 3650 (μ-OH), 2201 (C≡N), 1616 (C═N) cm^{-1}. HRMS (FAB^+): *m*/*z* 877.3287, calcd for $C_{48}H_{59}Cu_2N_6O_2$ 877.3491. Anal. Calcd for $C_{48}H_{58}Cu_2N_6O_2$: C, 65.65; H, 6.66; N, 9.57. Found: C, 65.64; H, 6.66; N, 9.55.

$[Cu^{II}(^{CN}L^{Dipp})(AcO)]$. Ligand $^{CN}L^{Dipp}H$ (41.6 mg, 0.1 mmol) in methanol (10 mL) was added into a methanol solution (10 mL) of $Cu^{II}(OAc)_2 \cdot H_2O$ (20.0 mg, 0.1 mmol). After addition of triethylamine (0.1 mmol), the mixture was refluxed for 48 h. The mixture was then concentrated and redissolved into 3 mL of methanol. The methanol solution was poured into ether (50 mL) to give green precipitates, which were collected by filtration and dried (77%). Single crystals suitable for X-ray crystallographic analysis were also obtained by vapor diffusion of ether into a CH_2Cl_2 solution of the complex. IR (KBr): 2185 (C≡N), 1616 (C═N) cm^{-1}. HRMS (FAB^+): *m*/*z* 478.2294, calcd for $C_{28}H_{37}CuN_3$ ($[Cu^{II}L]^+$) 478.2283. Anal. Calcd for $C_{30}H_{39}CuN_3O_2$: C, 67.08; H, 7.32; N, 7.82. Found: C, 67.31; H, 7.43; N, 7.67.

$[Cu^{II}(^{NO_2}L^{Ph})_2]$. Ligand $^{NO_2}L^{Ph}H$ (53.3 mg, 0.2 mmol) in methanol (10 mL) was added into a methanol solution (10 mL) of $Cu^{II}(OAc)_2 \cdot H_2O$ (20.0 mg, 0.1 mmol), and the mixture was stirred for 1 h at room temperature. The resulting precipitates were then collected by filtration and dried to obtain green powder in 88% yield. Single crystals suitable for X-ray crystallographic analysis were obtained by slow diffusion of liquid methanol into a CH_2Cl_2 solution containing the complex. IR (KBr) 1600 (C═N), 1582, 1530, 1490, 1483, 1315, 1274 (NO_2) cm^{-1}. HRMS (FAB^+): *m*/*z* 556.1216, calcd for $C_{30}H_{25}CuN_6O_4$ 596.1255. Anal. Calcd for $C_{30}H_{24}N_6O_4Cu$: C, 60.45; H, 4.06; N, 14.10. Found: C, 60.06; H, 3.95; N, 13.99.

$[Cu^{II}(^{NO_2}L^{Dtbp})_2]$. This compound was obtained in a similar manner described for the synthesis of $[Cu^{II}(^{NO_2}L^{Ph})_2]$ as green powder in 95% yield. Single crystals suitable for X-ray crystallographic analysis were obtained by slow diffusion of liquid methanol into a CH_2Cl_2 solution containing the complex. IR (KBr) 1595 (C═N), 1529, 1486, 1364, 1282 (NO_2) cm^{-1}. MS (FAB^+): *m*/*z* 1044.7 ($[Cu^{II}L_2 + H]^+$). Anal. Calcd for $C_{62}H_{90}N_6O_4Cu$: C, 71.26; H, 8.49; N, 8.04. Found: C, 71.07; H, 8.53; N, 8.02.

Scheme 1

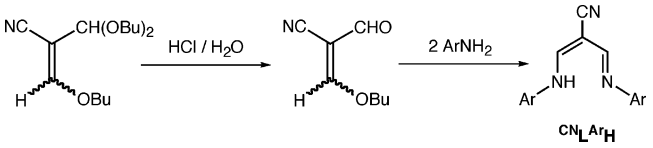

Scheme 2

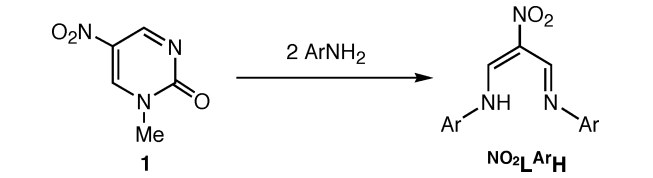

$[Cu^{II}_2(^{NO_2}L^{Mes})_2(\mu\text{-}OH)_2]$. Ligand $^{NO_2}L^{Mes}H$ (35.4 mg, 0.1 mmol) suspended in methanol (10 mL) was added to $Cu^{II}(OAc)_2 \cdot H_2O$ (20.0 mg, 0.1 mmol) in CH_3OH (10 mL) at 60 °C. Then, the mixture was refluxed for 24 h. Removal of the solvent gave brown material, from which the dicopper complex was isolated by recrystallization from CH_2Cl_2/hexane as purple microcrystals in a 95% yield. IR (KBr) 3640 (μ-OH), 1612 (C═N), 1603, 1531, 1477, 1373, 1299 (NO_2) cm^{-1}. MS (FAB^+) *m*/*z* 845.4 ($[(CuL)_2(\mu\text{-}OH)]^+$). Anal. Calcd for $C_{42}H_{50}N_6O_6Cu_2$: C, 58.52; H, 5.85; N, 9.75. Found: C, 58.27; H, 5.82; N, 9.62.

Results and Discussion

Ligand Synthesis and Characterization. Ligands $^{Me}L^{Ph}H$ and $^{H}L^{Ph}H$ were prepared according to the reported procedures.[7] The cyano derivatives $^{CN}L^{Ar}H$ (Ar = aryl group) were synthesized by following Noguchi's procedure with a little modification (Scheme 1).[11] The nitro derivatives $^{NO_2}L^{Ar}H$ (Ar = aryl group), on the other hand, were obtained from the reaction between 1-methyl-5-nitro-1*H*-pyrimidin-2-one (**1**) and the aniline derivatives (Scheme 2).[9] Crystal structures of $^{CN}L^{Mes}H$, $^{CN}L^{Dep}H$, $^{NO_2}L^{Mes}H$, and $^{NO_2}L^{Dtbp}H$ have been solved as shown in Figure 1, and their crystallographic data and selected bond length, bond angles, and angles of the least-squares planes are presented in Tables 1 and 2.

In the previous paper by Nishiwaki et al., the products of the reaction between **1** and amines were assigned as diimine derivatives **A** shown in Scheme 3. This assignment was based on magnetic equivalence of the two β-protons on the carbon framework as well as the two *N*-aromatic substituents in the ^1H and ^{13}C NMR spectra (for the definition of β-proton, see Chart 1).[9] Structural refinement of $^{NO_2}L^{Ar}H$ in the X-ray analysis [parts c and d in Figure 1], however, has unambiguously indicated that the compounds exist mainly as 3-imino-2-nitropropenylamine derivatives **B** (Scheme 3). The dissociable proton of each compound was found to be associated with one of the nitrogen atoms N(1), and the bond distances of C(1)−C(3) (1.451(4) and 1.436(3) Å for Ar = Mes and Dtbp, respectively) and C(2)−N(1) (1.308(5) and 1.317(3) Å) are longer than those of C(1)−C(2) (1.420(5) and 1.389 (3) Å) and C(3)−N(2) (1.285(4) and 1.283(3) Å), respectively (see, Table 2). Semiempirical molecular orbital calculations (PM3) of the compounds indicated that form **B** is much more stable than form **A**; ΔH_f values follow for $^{NO_2}L^{Ar}H$: Ar = Ph, form **A**, 85.7 kcal/mol, form **B**, 69.4 kcal/mol; Ar = Mes, form **A**, 38.5 kcal/mol, form **B**, 29.5

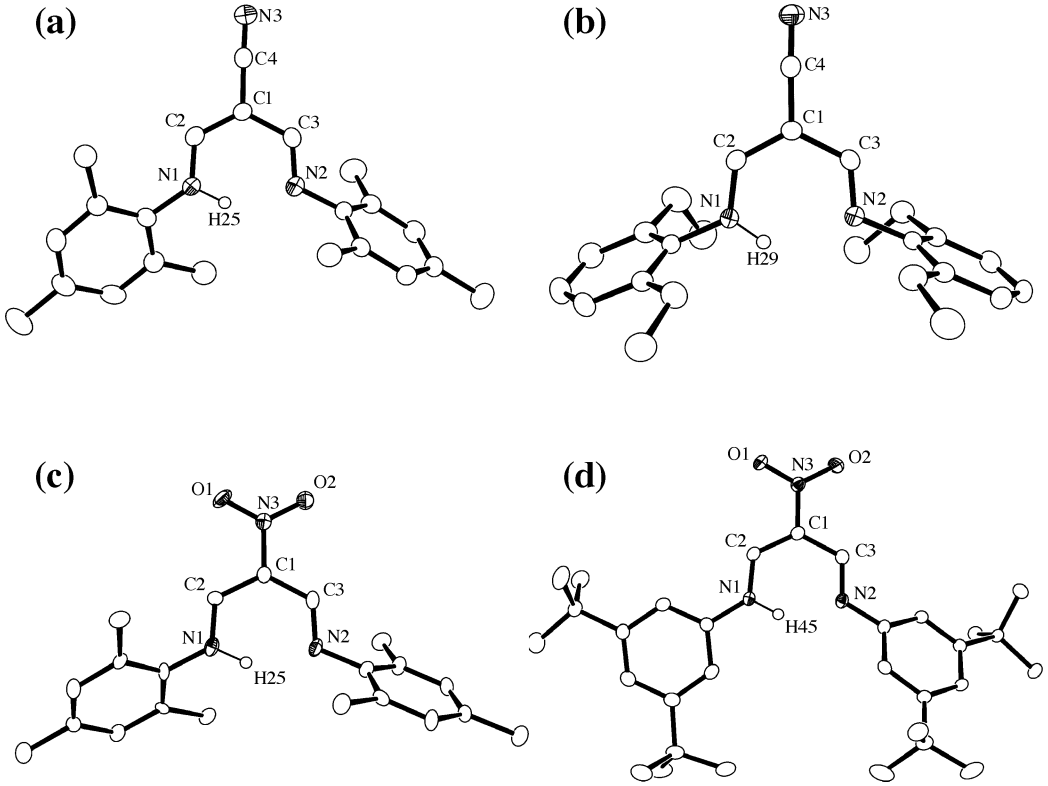

Figure 1. ORTEP drawings of (a) $^{CN}L^{Mes}H$ (molecule 1), (b) $^{CN}L^{Dep}H$, (c) $^{NO_2}L^{Mes}H$, and (d) $^{NO_2}L^{Dtbp}H$ with 50% probability thermal ellipsoids. Hydrogen atoms except the one at the amino group [H(25) of a, H(29) of b, H(25) of c, and H(45) of d] are omitted for clarity.

Table 1. Summary of X-ray Crystallographic Data of $^{CN}L^{Mes}H$, $^{CN}L^{Dep}H$, $^{NO_2}L^{Mes}H$, and $^{NO_2}L^{Dtbp}H$

	$^{CN}L^{Mes}H$	$^{CN}L^{Dep}H$	$^{NO_2}L^{Mes}H$	$^{NO_2}L^{Dtbp}H$
empirical formula	$C_{22}H_{25}N_3$	$C_{24}H_{29}N_3$	$C_{21}H_{25}N_3O_2$	$C_{31}H_{45}N_3O_2$
fw	331.46	359.51	351.45	491.72
cryst syst	monoclinic	monoclinic	triclinic	monoclinic
space group	$P2_1/n$ (No. 14)	$P2_1/n$ (No. 14)	$P\bar{1}$ (No. 2)	$P2_1/n$ (No. 14)
a, Å	15.4580(3)	8.9281(4)	8.954(2)	13.6374(4)
b, Å	15.5024(3)	19.8377(8)	14.536(4)	9.2069(3)
c, Å	16.1439(4)	11.7517(5)	8.220(2)	23.8174(9)
α, deg			105.55(1)	
β, deg	97.2594(9)	97.603(1)	109.61(1)	98.942(2)
γ, deg			77.70(2)	
V, Å^3	3837.7(1)	2063.1(2)	961.9(5)	2954.1(2)
Z	8	4	2	4
F(000)	1424.00	776.00	376.00	1072.00
D_{calcd}, g/cm^3	1.147	1.157	1.213	1.106
T, °C	−115	−115	−115	−115
cryst size, mm^3	0.20 × 0.25 × 0.30	0.10 × 0.20 × 0.20	0.30 × 0.30 × 0.30	0.20 × 0.30 × 0.30
μ(Mo Kα), cm^{-1}	0.68	0.68	0.79	0.69
radiation	Mo Kα (0.71069 Å)	Mo Kα (0.71069 Å)	Mo Kα (0.71069 Å)	Mo Kα (0.71069 Å)
$2\theta_{max}$, deg	55.0	54.8	54.9	55.0
no. reflns measd	33664	18839	6073	22656
no. reflns obsd	6242 [$I > 1.00\sigma(I)$]	3343 [$I > 3.00\sigma(I)$]	2717 [$I > 3.00\sigma(I)$]	3785 [$I > 3.00\sigma(I)$]
no. variables	502	290	261	371
R^a; $R_w{}^b$	0.066; 0.081	0.042; 0.048	0.077; 0.089	0.047; 0.053
GOF indicator	0.98	1.01	1.00	1.06

[a] $R = \Sigma||F_o| - |F_c||/\Sigma|F_o|$. [b] $R_w = [\Sigma w(|F_o| - |F_c|)^2/\Sigma wF_o^2]^{1/2}$.

kcal/mol; Ar = Dtbp, form **A**, −0.97 kcal/mol, form **B**, −17.9 kcal/mol. Thus, the magnetic equivalence of the β-proton of the carbon framework and the aromatic protons of the *N*-substituents in the NMR spectra can be explained by a rapid tautmerization within an NMR time scale between **B** and **B′** in solution as illustrated in Scheme 4.

Compounds $^{CN}L^{Ar}H$ have a similar structural feature of the ligand framework. Namely, the amine proton was found to exist at N(1), and the bond distances of C(1)−C(3) (1.442(5) and 1.442(2) Å for Ar = Mes and Dep, respectively) and C(2)−N(1) (1.326(4) and 1.323(2) Å) are longer than those of C(1)−C(2) (1.386(5) and 1.383(2) Å) and C(3)−N(2) (1.291(4) and 1.275(2) Å), respectively (see, Table 2). Detailed comparison of the crystal structures between $^{CN}L^{Mes}H$ [Figure 1a] and $^{NO_2}L^{Mes}H$ [Figure 1c] having the same aromatic substituent (Mes) indicates that the bond lengths of C(1)−C(2) and C(1)−C(3) of $^{NO_2}L^{Mes}H$ (1.420(5) and 1.451(4) Å) are longer than those of $^{CN}L^{Mes}H$

Table 2. Selected Bond Lengths (Å), Angles (deg), and Angles of Least Square Planes (deg) of $^{CN}L^{Mes}H$, $^{CN}L^{Dep}H$, $^{NO_2}L^{Mes}H$, and $^{NO_2}L^{Dtbp}H$[a]

$^{CN}L^{Mes}H$			$^{CN}L^{Dep}H$		$^{NO_2}L^{Mes}H$		$^{NO_2}L^{Dtbp}H$	
	molecule 1	molecule 2						
N(3)−C(4)	1.148(4)	1.148(4)	N(3)−C(4)	1.148(2)	O(1)−N(3)	1.261(4)	O(1)−N(3)	1.242(2)
N(1)−C(2)	1.326(4)	1.313(4)	N(1)−C(2)	1.323(2)	O(2)−N(3)	1.258(4)	O(2)−N(3)	1.239(2)
N(2)−C(3)	1.291(4)	1.291(4)	N(2)−C(3)	1.275(2)	N(1)−C(2)	1.308(5)	N(1)−C(2)	1.317(3)
N(1)−C(5)	1.424(4)	1.437(4)	N(1)−C(5)	1.438(2)	N(1)−C(4)	1.444(4)	N(1)−C(4)	1.417(3)
N(2)−C(14)	1.420(4)	1.434(4)	N(2)−C(15)	1.421(2)	N(2)−C(3)	1.285(4)	N(2)−C(3)	1.283(3)
C(1)−C(2)	1.386(5)	1.393(5)	C(1)−C(2)	1.383(2)	N(2)−C(13)	1.457(4)	N(2)−C(18)	1.418(3)
C(1)−C(3)	1.442(5)	1.424(5)	C(1)−C(3)	1.442(2)	N(3)−C(1)	1.416(4)	N(3)−C(1)	1.431(3)
C(1)−C(4)	1.429(5)	1.425(5)	C(1)−C(4)	1.425(2)	C(1)−C(2)	1.420(5)	C(1)−C(2)	1.389(3)
					C(1)−C(3)	1.451(4)	C(1)−C(3)	1.436(3)
C(2)−N(1)−C(5)	129.1(3)	123.8(3)	C(2)−N(1)−C(5)	121.6(1)	C(2)−N(1)−C(4)	123.3(3)	C(2)−N(1)−C(4)	128.1(2)
C(3)−N(2)−C(14)	120.8(3)	119.7(3)	C(3)−N(2)−C(15)	118.5(1)	C(3)−N(2)−C(13)	117.7(3)	C(3)−N(2)−C(18)	122.8(2)
N(3)−C(4)−C(1)	178.0(4)	178.3(4)	N(3)−C(4)−C(1)	177.8(2)	O(1)−N(3)−O(2)	122.6(3)	O(1)−N(3)−O(2)	122.5(2)
C(2)−C(1)−C(4)	118.9(3)	118.3(3)	C(2)−C(1)−C(4)	118.0(1)	O(1)−N(3)C(1)	119.1(3)	O(1)−N(3)−C(1)	119.2(2)
C(3)−C(1)−C(4)	117.4(3)	118.7(3)	C(3)−C(1)−C(4)	118.2(1)	O(2)−N(3)−C(1)	118.3(3)	O(2)−N(3)−C(1)	118.3(2)
C(2)−C(1)−C(3)	123.6(3)	123.1(3)	C(2)−C(1)−C(3)	123.7(1)	N(3)−C(1)−C(2)	116.3(3)	N(3)−C(1)−C(2)	116.6(2)
N(1)−C(2)−C(1)	121.7(3)	123.0(3)	N(1)−C(2)−C(1)	125.5(1)	N(3)−C(1)−C(3)	118.6(3)	N(3)−C(1)−C(3)	118.8(2)
N(2)−C(3)−C(1)	121.9(3)	122.6(3)	N(2)−C(3)−C(1)	122.2(1)	C(2)−C(1)−C(3)	125.1(3)	C(2)−C(1)−C(3)	124.6(2)
					N(1)−C(2)−C(1)	121.7(3)	N(1)−C(2)−C(1)	122.0(2)
					N(2)−C(3)−C(1)	121.2(3)	N(2)−C(3)−C(1)	119.2(2)
plane 1−plane 2	32.83°	84.36°	plane 1−plane 2	71.13°	plane 1−plane 2	49.06°	plane 1−plane 2	3.62°
plane 1−plane 3	61.14°	88.72°	plane 1−plane 3	78.13°	plane 1−plane 3	65.38°	plane 1−plane 3	39.11°
plane 2−plane 3	75.74°	61.93°	plane 2−plane 3	50.30°	plane 2−plane 3	79.60°	plane 2−plane 3	40.25°

[a] Estimated standard deviations are given in parentheses. Definitions of the least-squares planes follow. For $^{CN}L^{Mes}H$: plane 1, N(1)−N(2)−C(1)−C(2)−C(3); plane 2, C(5)−C(6)−C(7)−C(8)−C(9)−C(10); plane 3, C(14)−C(15)-C(16)−C(17)−C(18)−C(19). For $^{CN}L^{Dep}H$: plane 1, N(1)−N(2)−C(1)−C(2)−C(3); plane 2, C(5)−C(6)−C(7)−C(8)−C(9)−C(10); plane 3, C(15)−C(16)−C(17)−C(18)−C(19)−C(20). For $^{NO_2}L^{Mes}H$: plane 1, N(1)−N(2)−C(1)−C(2)−C(3); plane 2, C(4)−C(5)−C(6)−C(7)−C(8)−C(9); plane 3, C(13)−C(14)−C(15)−C(16)−C(17)−C(18). For $^{NO_2}L^{Dtbp}H$: plane 1, N(1)−N(2)−C(1)−C(2)−C(3); plane 2, C(4)−C(5)−C(6)−C(7)−C(8)−C(9); plane 3, C(18)−C(19)−C(20)−C(21)−C(22)−C(23).

Scheme 3

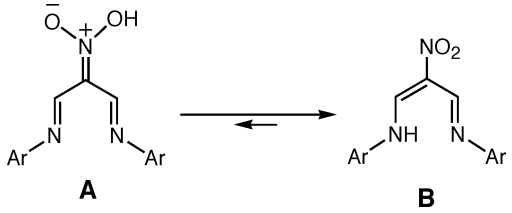

Scheme 4

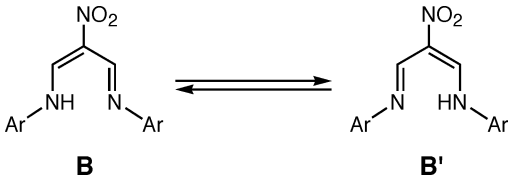

(1.386(5) and 1.442(5) Å for molecule 1, 1.393(5) and 1.424(5) Å for molecule 2), while bond lengths of N(1)−C(2) and N(2)−C(3) of $^{NO_2}L^{Mes}H$ (1.308(5) and 1.285(4) Å) are shorter than those of $^{CN}L^{Mes}H$ (1.326(4) and 1.291(4) Å for molecule 1, 1.313(4) and 1.437(4) Å for molecule 2). These results clearly suggest that, in the nitro derivative, the double bond character of C(1)−C(2) and C(1)−C(3) decreases while that of N(1)−C(2) and N(2)−C(3) increases as compared to that of the corresponding bonds in the cyano derivative. Thus, it could be concluded that there is some contribution of the diimine form **A** (Scheme 3) to the overall structure in the nitro derivative $^{NO_2}L^{Mes}H$.

It is also interesting to note that the angles between the least-squares plane defined by N(1)−C(2)−C(1)−C(3)−N(2) and the aromatic rings of the *N*-aryl groups in $^{NO_2}L^{Dtbp}H$ are smaller than those of other compounds. This could be attributed to the steric effects of the *o*-substituents in Mes and Dep. Namely, the steric repulsion between the *o*-substituents of Mes and Dep in $^{CN}L^{Mes}H$, $^{CN}L^{Dep}H$ and $^{NO_2}L^{Mes}H$ and the *β*-proton of the ligand framework makes the torsion angle larger than that in $^{NO_2}L^{Dtbp}H$, which does not have the *o*-substituents in the *N*-aryl group (Dtbp). Such a steric effect also affected the structures of the copper(II) complexes as discussed in following paragraphs.

Bis(*β*-diketiminate) Copper(II) Complexes. Treatment of $Cu^{II}(OAc)_2$ with the neutral ligands carrying phenyl (Ph) or 3,5-di-*tert*-butylphenyl (Dtbp) groups as the aromatic substituent ($^{Me}L^{Ph}H$, $^{H}L^{Ph}H$, $^{CN}L^{Ph}H$, $^{NO_2}L^{Ph}H$, and $^{NO_2}L^{Dtbp}H$) in methanol gave the corresponding bis(*β*-diketiminate) copper(II) complexes, the crystal structures of which, except the complex of $^{Me}L^{Ph}H$, have been determined by X-ray crystallographic analysis as shown in Figure 2. The crystallographic data and selected bond lengths and angles as well as torsion angles of the two coordination planes defined by N−Cu−N are given in Tables 3 and 4. Although a number of bis(*β*-diketiminate) copper(II) complexes have so far been reported,[8−17] there is only one precedent for the X-ray structure of bis(*β*-diketiminate) copper(II) complex, which is supported by $^{CHO}L^{Dmp}$ [R^1 = CHO; R^3 = Dmp (3,5-dimethylphenyl)].[17]

The copper(II) complexes exhibit distorted tetrahedral geometries, where the dihedral angles between the two coordination planes are 63.68°, 62.48°, 62.03°, and 61.39° and the mean values of Cu−N bond length are 1.951, 1.959,

(12) Honeybourne, C. L.; Webb, G. A. *J. Chem. Soc., Chem. Commun.* **1968**, 739−740.
(13) McGeachin, S. G. *Can. J. Chem.* **1968**, *46*, 1903−1912.
(14) Attanasio, D.; Tomlison, A. G.; Alagna, L. *J. Chem. Soc., Chem. Commun.* **1977**, 618−619.
(15) Nishida, Y.; Oishi, N.; Kida, S. *Inorg. Chim. Acta* **1979**, *32*, 7−10.
(16) Kulichenko, A. V.; Kurbatov, V. P.; Kukharicheva, E. S.; Osipov, O. A. *J. Gen. Chem. USSR* **1987**, *55*, 612−615.
(17) Knorr, R.; Zölch, R.; Polborn, K. *Heterocycles* **1995**, *40*, 559−576.

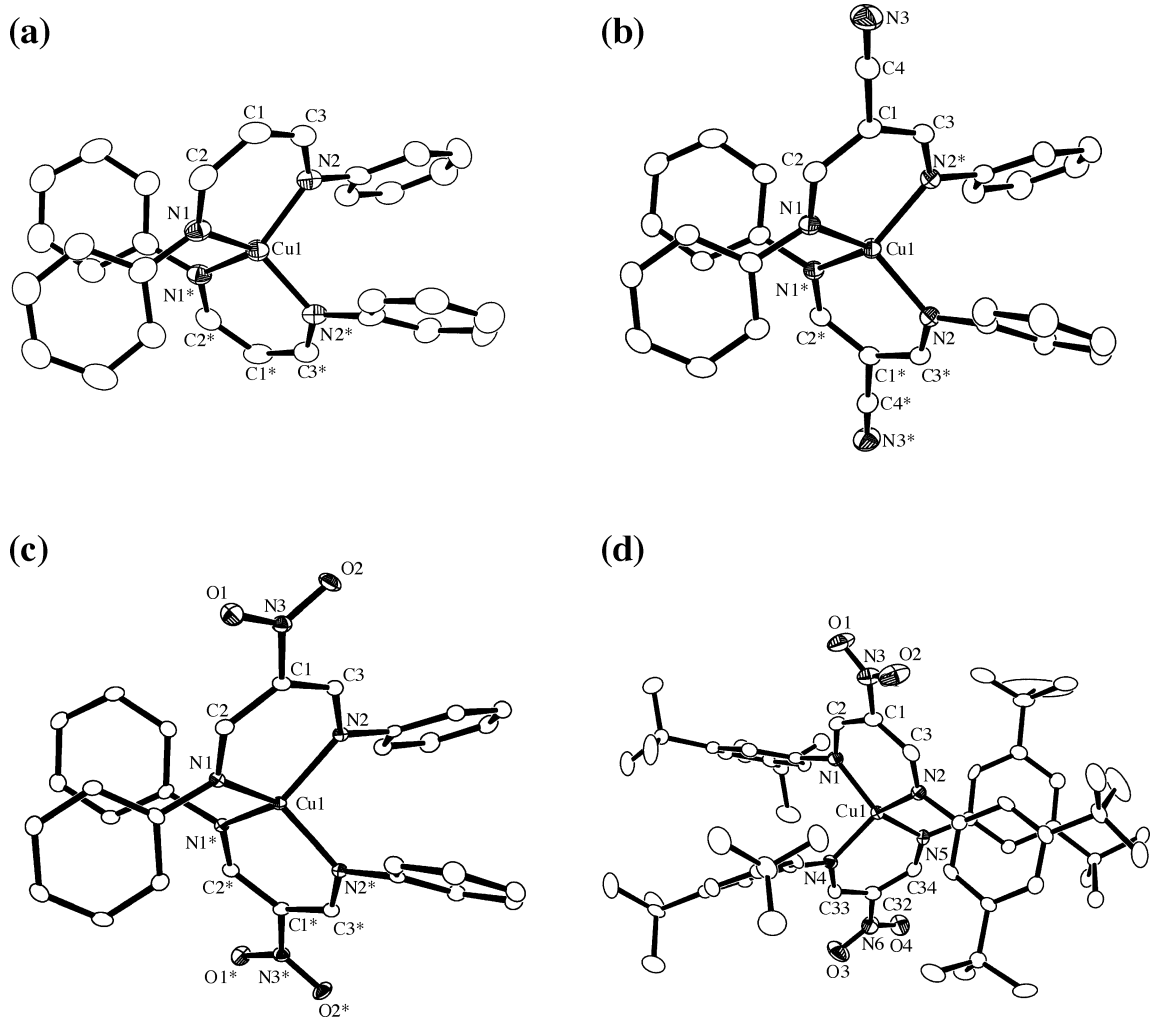

Figure 2. ORTEP drawings of (a) $[Cu^{II}(^{H}L^{Ph})_2]$, (b) $[Cu^{II}(^{CN}L^{Ph})_2]$, (c) $[Cu^{II}(^{NO_2}L^{Ph})_2]$, and (d) $[Cu^{II}(^{NO_2}L^{Dtbp})_2]$ with 50% probability thermal ellipsoids. Hydrogen atoms are omitted for clarity.

1.952, and 1.966 Å for $[Cu^{II}(^{H}L^{Ph})_2]$, $[Cu^{II}(^{CN}L^{Ph})_2]$, $[Cu^{II}(^{NO_2}L^{Ph})_2]$, and $[Cu^{II}(^{NO_2}L^{Dtbp})_2]$, respectively (Table 4). These structural parameters are nearly the same to those of the bis(β-diketiminate) copper(II) complex supported by $^{CHO}L^{Dmp}$ [dihedral angle = 62.4°; $Cu-N_{av}$ = 1.952 Å].[17] Thus, the electronic nature of substituent R^1 and the *meta*-substituents of the *N*-aromatic groups (Me in $^{CHO}L^{Dmp}$ and *t*-Bu in $^{NO_2}L^{Dtbp}$) hardly affect the core structure of the bis(β-diketiminate) copper(II) complexes.

Spectral data of the bis(β-diketiminate) copper(II) complexes are summarized in Table 5. The complexes exhibit ESR spectra having $g_{\|} = 2.182-2.214$, $g_{\perp} = 2.054-2.056$, and $A_{\|} = 125-132$ G. These ESR parameters are also nearly the same to those of the bis(β-diketiminate) copper(II) complexes so far reported.[13,15] The smaller $A_{\|}$ values, as compared to that of square planar copper(II) complexes, are characteristic of tetrahedrally distorted bis(β-diketiminate) copper(II) complexes.[13,15] Thus, the similarity in the $A_{\|}$ value clearly indicates that the structures of the copper(II) complexes in solution are also very close each other as in the case of the crystal structures (Figure 2).[18] In such a case, the differences in $g_{\|}$ values could mainly be attributed to the electronic effects of the ligand substituents. As can be seen in Table 5, the $g_{\|}$ values increase as the electron-withdrawing nature of R^1 increases in the series of $[Cu^{II}(^{R1}L^{Ph})_2]$ (R^1 = Me, H, CN, and NO_2, R^3 = Ph), although the $g_{\perp}$ values are rather constant (2.054−2.056). Thus, it can be said that the $g_{\|}$ values are correlated to the electron-donor ability of the β-diketiminate ligands, where the more electron-donor ability of the ligand, the smaller the $g_{\|}$ value of copper(II) ion.[19]

The electronic spectrum in THF is also sensitive to the electron-donor ability of the ligands (Table 5). Although complete assignments of the absorption bands have yet to be accomplished, the following peak assignments are possible.[19] The strong absorption bands ($\epsilon > 10^4$ M^{-1} cm^{-1}) below 500 nm could be attributed to $\pi-\pi^*$ transitions of the β-diketiminate ligands, since similar absorption bands also exist in the zinc(II) complexes supported by the same ligands.[20] Then, the reasonably intense bands in the visible

(18) The ESR parameters of the bis(β-diketiminate) copper(II) complexes in CH_2Cl_2 are nearly the same as those of the complexes in THF (Table 5), indicating that the solvent molecules do not coordinate to the metal center in the THF solution.

(19) Theoretical studies are planned to be carried out in order to evaluate the substituent effects on the spectroscopic features of bis(β-diketiminate) copper(II) complexes in more detail.

Table 3. Summary of X-ray Crystallographic Data of $[Cu^{II}(^{H}L^{Ph})_2]$, $[Cu^{II}(^{CN}L^{Ph})_2]$, $[Cu^{II}(^{NO_2}L^{Ph})_2]$, $[Cu^{II}(^{NO_2}L^{Dtbp})_2]$, $[Cu^{II}_2(^{CN}L^{Mes})_2(\mu\text{-}OH)_2]$, $[Cu^{II}_2(^{CN}L^{Dep})_2(\mu\text{-}OH)_2]$, and $[Cu^{II}(^{CN}L^{Dipp})(AcO)]$

	$[Cu^{II}(^{H}L^{Ph})_2]$	$[Cu^{II}(^{CN}L^{Ph})_2]$	$[Cu^{II}(^{NO_2}L^{Ph})_2]$	$[Cu^{II}(^{NO_2}L^{Dtbp})_2]$	$[Cu^{II}_2(^{CN}L^{Mes})_2$-$(\mu\text{-}OH)_2]$	$[Cu^{II}_2(^{CN}L^{Dep})_2$-$(\mu\text{-}OH)_2]$	$[Cu^{II}_2(^{CN}L^{Dipp})$-(AcO)]
empirical formula	$C_{30}H_{26}CuN_4$	$C_{32}H_{24}CuN_6$	$C_{30}H_{24}CuN_6O_4$	$C_{62}H_{88}CuN_6O_4$	$C_{44}H_{50}Cu_2N_6O_2$	$C_{48}H_{58}Cu_2N_6O_2$	$C_{30}H_{39}CuN_3O_2$
fw	506.11	556.13	596.10	1044.96	822.01	878.12	537.20
cryst syst	orthorhombic	monoclinic	monoclinic	monoclinic	monoclinic	triclinic	orthorhombic
space group	*Aba*2 (No. 41)	*C*2/*c* (No. 15)	*C*2/*c* (No. 15)	$P2_1/c$ (No. 14)	$P2_1/n$ (No. 14)	$P\bar{1}$ (No. 2)	*Pnma* (No. 62)
a, Å	14.19(2)	7.2391(3)	7.64143(4)	15.8197(5)	15.564(2)	9.465(1)	12.435(2)
b, Å	7.087(8)	23.0260(9)	23.016(2)	19.2852(6)	14.764(2)	11.151(2)	21.398(4)
c, Å	23.76(4)	15.5591(8)	14.995(1)	20.0849(5)	17.723(3)	11.601(1)	10.729(2)
α, deg						67.824(4)	
β, deg		97.720(4)	102.931(3)	98.766(2)	94.324(6)	83.156(3)	
γ, deg						74.441(7)	
V, Å^3	2388.9(5)	2570.0(2)	2561.2(3)	6056.1(3)	4060.8(1)	1092.0(2)	2854.8(9)
Z	4	4	4	4	4	1	4
F(000)	1052.00	1148.00	1228.00	2252.00	1720.00	462.00	1140.00
D_{calcd}, g/cm^3	1.407	1.437	1.546	1.146	1.344	1.335	1.250
T, °C	−115	−115	−115	−115	−115	−115	−115
cryst size, mm^3	0.10 × 0.15 × 0.15	0.10 × 0.10 × 0.30	0.10 × 0.10 × 0.20	0.20 × 0.20 × 0.20	0.30 × 0.30 × 0.30	0.20 × 0.20 × 0.30	0.20 × 0.20 × 0.30
μ(Mo Kα), cm^{-1}	9.41	8.84	9.04	4.09	10.91	10.19	7.95
radiation	Mo Kα (0.71069 Å)	Mo Kα (0.71069 Å)	Mo Kα (0.71069 Å)	Mo Kα (0.71069 Å)	Mo Kα (0.71069 Å)	Mo Kα (0.71069 Å)	Mo Kα (0.71069 Å)
$2\theta_{max}$, deg	54.8	54.9	55.0	55.0	55.0	55.0	55.0
no. reflns measd	11440	11271	11885	25017	37161	10416	27321
no. reflns obsd	1119 [$I > 1.00\sigma(I)$]	2208 [$I > 3.00\sigma(I)$]	2443 [$I > 3.00\sigma(I)$]	8845 [$I > 1.00\sigma(I)$]	6019 [$I > 3.00\sigma(I)$]	4180 [$I > 3.00\sigma(I)$]	2027 [$I > 3.00\sigma(I)$]
no. variables	173	190	199	747	538	292	194
R;[a] R_w[b]	0.024; 0.048	0.031; 0.060	0.030; 0.042	0.059; 0.065	0.037; 0.039	0.030; 0.034	0.024; 0.036
GOF indicator	1.03	1.18	1.04	1.03	0.98	0.95	1.03

[a] $R = \sum||F_o| - |F_c||/\sum|F_o|$. [b] $R_w = [\sum w(|F_o| - |F_c|)^2/\sum wF_o^2]^{1/2}$.

region could be assigned to n−π* transitions of the ligands as well as ligand-to-metal charge transfer transitions (LMCT) of the copper(II) complex, those of which may overlap with the d−d bands of copper(II) as discussed in following paragraphs.

It has been documented that the distorted tetrahedral copper(II) complexes exhibit three d−d bands due to the $d_{z^2} \rightarrow d_{xy}$, $d_{x^2-y^2} \rightarrow d_{xy}$, and $d_{xz}, d_{yz} \rightarrow d_{xy}$ transitions.[21] According to the previous report by Nishida et al.,[15] the weak $d_{z^2} \rightarrow d_{xy}$ and $d_{x^2-y^2} \rightarrow d_{xy}$ bands become obscure due to overlap with the relatively intense LMCT bands around 650−750 nm ($\epsilon \sim 10^3$ M^{-1} cm^{-1}, Table 5). Thus, only the $d_{xz}, d_{yz} \rightarrow d_{xy}$ transition bands in the near-IR region can be evaluated.[15] Apparently, the d−d absorption bands in the near-IR region shift toward a shorter wavelength (blue-shift) as the electron-withdrawing nature of R^1 increases in the series of $[Cu^{II}(^{R1}L^{Ph})_2]$ (R^1 = Me, H, CN, and NO_2, R^3 = Ph). On the other hand, this band shifts toward longer wavelength (red-shift), when the R^3 substituent (Ph) is replaced by the more electron-donating substituent Dtbp ($[Cu^{II}(^{NO_2}L^{Ph})_2]$ vs $[Cu^{II}(^{NO_2}L^{Dtbp})_2]$, Table 5). Since the coordination geometry of the copper(II) center is nearly the same among the bis(β-diketiminate) complexes as demonstrated by the ESR (Table 5) and the X-ray crystallographic analysis (Table 4), the shifts of the d−d band can be mainly attributed to the electronic effects of R^1 and R^3. We assume that electron donation from the β-diketiminate ligand through σ-antibonding interactions between the d orbitals (d_{xz} and d_{yz}) of copper and the p orbitals of the ligand causes an increase of the energy level of d_{xz} and d_{yz} orbitals, which on the other hand decreases the transition energy of $d_{xz}, d_{yz} \rightarrow d_{xy}$. Thus, the ligand with the electron-donating substituent such as $^{Me}L^{Ph-}$ causes the red-shift of the d−d band as compared to the corresponding ligands with the electron-withdrawing substituent such as $^{CN}L^{Ph-}$ and $^{NO_2}L^{Ph-}$.[19] The red-shift of the d−d band in $[Cu^{II}(^{NO_2}L^{Dtbp})_2]$ (1305 nm) as compared to that of $[Cu^{II}(^{NO_2}L^{Ph})_2]$ (1200 nm) can also be attributed to the increasing electron-donating ability of Dtbp as compared to that of Ph.[19]

In Figure 3 is shown the cyclic voltammograms of $[Cu^{II}(^{Me}L^{Ph})_2]$, $[Cu^{II}(^{H}L^{Ph})_2]$, $[Cu^{II}(^{CN}L^{Ph})_2]$, and $[Cu^{II}(^{NO_2}L^{Ph})_2]$ in THF. Complexes $[Cu^{II}(^{Me}L^{Ph})_2]$ and $[Cu^{II}(^{H}L^{Ph})_2]$ gave irreversible reduction peak at significantly negative positions at −1.62 and −1.46 V versus Fc/Fc$^+$, respectively [parts a and b in Figure 3], while $[Cu^{II}(^{CN}L^{Ph})_2]$ and $[Cu^{II}(^{NO_2}L^{Ph})_2]$ exhibited reversible redox couples at −0.97 and −0.68 V versus Fc/Fc$^+$, respectively [parts c and d in Figure 3]. Complex $[Cu^{II}(^{NO_2}L^{Dtbp})_2]$ also provides a reversible redox couple at −0.71 V, which is a little negative as compared to that of $[Cu^{II}(^{NO_2}L^{Ph})_2]$ (not shown in Figure 3). Apparently, the reduction potentials as well as reversibility of the redox processes are significantly affected by the ligand substituent R^1. The positive shift of the reduction potential on going from $[Cu^{II}(^{Me}L^{Ph})_2]$ to $[Cu^{II}(^{NO_2}L^{Ph})_2]$ can be attributed to the increase of electron-withdrawing ability of R^1. The slight negative shift of $E_{1/2}$ of $[Cu^{II}(^{NO_2}L^{Dtbp})_2]$ as compared to that of $[Cu^{II}(^{NO_2}L^{Ph})_2]$, on the other hand, is due to the increasing electron-donor ability of the aromatic substituent Dtbp as already discussed. Irreversibility observed in the redox

(20) Synthesis and characterization of the zinc(II) complexes will be reported elsewhere.

(21) (a) Ferguson, J. *J. Chem. Phys.* **1964**, *40*, 822−830. (b) Smith, D. W. *J. Chem. Soc. A* **1970**, 2900−2902. (c) Smith, D. W. *Inorg. Chim. Acta* **1977**, *22*, 107−110.

Table 4. Selected Bond Lengths (Å), Angles (deg), and Angles of Least Square Planes (deg) of $[Cu^{II}(^{H}L^{Ph})_2]$, $[Cu^{II}(^{CN}L^{Ph})_2]$, $[Cu^{II}(^{NO_2}L^{Ph})_2]$, $[Cu^{II}(^{NO_2}L^{Dtbp})_2][Cu^{II}_2(^{CN}L^{Mes})_2(\mu\text{-}OH)_2]$, $[Cu^{II}_2(^{CN}L^{Dep})_2(\mu\text{-}OH)_2]$, and $[Cu^{II}(^{CN}L^{Dipp})(AcO)]$[a]

$[Cu^{II}(^{H}L^{Ph})_2]$		$[Cu^{II}(^{CN}L^{Ph})_2]$		$[Cu^{II}(^{NO_2}L^{Ph})_2]$		$[Cu^{II}(^{NO_2}L^{Dtbp})_2]$			
Cu(1)−N(1)	1.971(4)	Cu(1)−N(1)	1.954(3)	Cu(1)−N(1)	1.944(2)	Cu(1)−N(1)	1.975(3)	Cu(1)−N(2)	1.946(3)
Cu(1)−N(2)	1.931(4)	Cu(1)−N(2)	1.964(3)	Cu(1)−N(2)	1.959(2)	Cu(1)−N(4)	1.957(3)	Cu(1)−N(5)	1.974(3)
N(1)−C(2)	1.321(5)	N(1)−C(2)	1.310(5)	N(1)−C(2)	1.308(3)	N(1)−C(2)	1.310(5)	N(2)−C(3)	1.305(5)
N(1)−C(4)	1.415(5)	N(1)−C(5)	1.431(5)	N(1)−C(4)	1.424(3)	N(1)−C(4)	1.440(4)	N(2)−C(18)	1.445(4)
N(2)−C(3)	1.318(5)	N(2)−C(3)	1.306(4)	N(2)−C(3)	1.306(3)	C(1)−C(2)	1.402(5)	C(1)−C(3)	1.418(5)
N(2)−C(10)	1.415(6)	N(2)−C(11)	1.427(5)	N(2)−C(10)	1.427(3)	N(1)−Cu(1)−N(2)	94.2(1)	N(1)−Cu(1)−N(4)	103.4(1)
C(1)−C(2)	1.410(6)	C(1)−C(2)	1.406(5)	C(1)−C(2)	1.396(3)	N(2)−Cu(1)−N(4)	136.7(1)	N(1)−Cu(1)−N(5)	135.5(1)
C(1)−C(3)	1.379(6)	C(1)−C(3)	1.407(5)	C(1)−C(3)	1.412(3)	N(2)−Cu(1)−N(5)	100.7(1)	N(4)−Cu(1)−N(5)	93.9(1)
N(1)−Cu(1)−N(2)	96.1(2)	N(1)−Cu(1)−N(2)*	95.40(12)	N(1)−Cu(1)−N(2)	96.20(7)	Cu(1)−N(1)−C(2)	124.1(2)	Cu(1)−N(1)−C(4)	119.7(2)
Cu(1)−N(1)−C(2)	122.3(3)	Cu(1)−N(1)−C(2)	123.3(3)	Cu(1)−N(1)−C(2)	123.3(2)	C(2)−N(1)−C(4)	116.1(3)	Cu(1)−N(2)−C(3)	126.3(3)
Cu(1)−N(1)−C(4)	118.0(2)	Cu(1)−N(1)−C(5)	118.9(2)	Cu(1)−N(1)−C(4)	118.8(1)	Cu(1)−N(2)−C(18)	118.2(3)	C(3)−N(2)−C(18)	115.1(3)
C(2)−N(1)−C(4)	119.5(3)	C(2)−N(1)−C(5)	117.8(3)	C(2)−N(1)−C(4)	117.8(2)	Cu(1)−N(4)−C(33)	124.7(2)	Cu(1)−N(4)−C(35)	119.4(2)
Cu(1)−N(2)−C(3)	123.5(3)	Cu(1)−N(2)*−C(3)	124.3(3)	Cu(1)−N(2)−C(3)	123.8(2)	C(33)−N(4)−C(35)	115.9(3)	Cu(1)−N(5)−C(34)	124.7(3)
Cu(1)−N(2)−C(10)	117.5(3)	Cu(1)−N(2)−C(11)	116.9(2)	Cu(1)−N(2)−C(10)	117.2(1)	Cu(1)−N(5)−C(49)	118.1(2)	C(34)−N(5)−C(49)	117.1(3)
C(3)−N(2)−C(10)	118.8(3)	C(3)*−N(2)−C(11)	118.4(3)	C(3)−N(2)−C(10)	118.8(2)	N(3)−C(1)−C(2)	117.1(3)	N(3)−C(1)−C(3)	115.9(3)
C(2)−C(1)−C(3)	126.7(3)	C(2)−C(1)−C(3)	126.4(3)	C(2)−C(1)−C(3)	128.3(2)	C(2)−C(1)−C(3)	126.8(4)	N(1)−C(2)−C(1)	125.1(3)
N(1)−C(2)−C(1)	125.3(4)	N(1)−C(2)−C(1)	126.0(3)	N(1)−C(2)−C(1)	124.7(2)	N(2)−C(3)−C(1)	123.4(4)	N(1)−C(4)−C(5)	117.3(3)
N(2)−C(3)−C(1)	125.9(3)	N(2)*−C(3)−C(1)	124.6(3)	N(2)−C(3)−C(1)	123.5(2)	N(1)−C(4)−C(9)	122.2(3)	C(5)−C(4)−C(9)	120.4(3)
plane 1−plane 2	63.68°	plane 1−plane 2	62.48°	plane 1−plane 2	62.03°	plane 1−plane 2	61.39°		

$[Cu^{II}_2(^{CN}L^{Mes})_2(\mu\text{-}OH)_2]$				$[Cu^{II}_2(^{CN}L^{Dep})_2(\mu\text{-}OH)_2]$		$[Cu^{II}(^{CN}L^{Dipp})(AcO)]$	
Cu(1)−Cu(2)	2.981(1)	Cu(1)−O(1)	1.905(2)	Cu(1)−Cu(1)*	3.045(1)	Cu(1)−O(1)	2.028(1)
Cu(1)−O(2)	1.922(2)	Cu(1)−N(1)	1.959(3)	Cu(1)−O(1)	1.908(1)	Cu(1)−N(1)	1.944(2)
Cu(1)−N(2)	1.946(3)	Cu(2)−O(1)	1.919(2)	Cu(1)−O(1)*	1.926(1)	Cu(1)−C(16)	2.362(3)
Cu(2)−O(2)	1.920(2)	Cu(2)−N(4)	1.961(3)	Cu(1)−N(1)	1.955(2)	O(1)−C(16)	1.265(2)
Cu(2)−N(5)	1.963(3)	O(1)−O(2)	2.374(3)	Cu(1)−N(2)	1.943(2)	N(1)−C(2)	1.304(2)
N(1)−C(2)	1.303(4)	N(1)−C(5)	1.442(4)	O(1)−O(1)*	2.331(3)	N(1)−C(4)	1.450(2)
N(2)−C(3)	1.309(4)	N(2)−C(14)	1.443(4)	N(1)−C(2)	1.312(2)	C(1)−C(2)	1.418(2)
N(4)−C(24)	1.302(4)	N(4)−C(27)	1.441(4)	N(1)−C(5)	1.441(2)	C(16)−C(17)	1.493(4)
N(5)−C(25)	1.293(4)	N(5)−C(36)	1.442(4)	N(2)−C(3)	1.304(2)		
C(1)−C(2)	1.408(5)	C(1)−C(3)	1.411(5)	N(2)−C(15)	1.447(2)		
C(23)−C(24)	1.406(5)	C(23)−C(25)	1.414(4)	C(1)−C(2)	1.405(3)		
O(1)−Cu(1)−O(2)	76.7(1)	O(1)−Cu(1)−N(1)	94.3(1)	C(1)−C(3)	1.410(3)		
O(1)−Cu(1)−N(2)	169.5(1)	O(2)−Cu(1)−N(1)	170.8(1)	O(1)−Cu(1)−N(1)	96.02(6)	O(1)−Cu(1)−O(1)*	64.70(8)
O(2)−Cu(1)−N(2)	95.9(1)	N(1)−Cu(1)−N(2)	93.3(1)	O(1)−Cu(1)−N(2)	170.36(6)	O(1)−Cu(1)−N(1)	98.82(6)
O(1)−Cu(2)−O(2)	76.4(1)	O(1)−Cu(2)−N(4)	173.3(1)	N(1)−Cu(1)−N(2)	93.62(7)	N(1)−Cu(1)−N(1)*	94.79(9)
O(1)−Cu(2)−N(5)	93.8(1)	O(2)−Cu(2)−N(4)	97.2(1)	Cu(1)−O(1)−Cu(1)*	105.13(7)	N(1)−Cu(1)−C(16)	130.02(5)
O(2)−Cu(2)−N(5)	167.7(1)	N(4)−Cu(2)−N(5)	92.8(1)	Cu(1)−N(1)−C(2)	123.7(1)	Cu(1)−O(1)−C(16)	88.5(1)
Cu(1)−O(1)−Cu(2)	102.4(1)	Cu(1)−O(2)−Cu(2)	101.8(1)	Cu(1)−N(1)−C(5)	120.8(1)	Cu(1)−N(1)−C(2)	124.2(1)
Cu(1)−N(1)−C(2)	121.4(2)	Cu(1)−N(1)−C(5)	120.8(2)	C(2)−N(1)−C(5)	115.5(2)	Cu(1)−N(1)−C(4)	118.8(1)
C(2)−N(1)−C(5)	117.3(3)	Cu(1)−N(2)−C(3)	122.4(2)	Cu(1)−N(2)−C(3)	124.5(1)	C(2)−N(1)−C(4)	116.9(2)
Cu(1)−N(2)−C(14)	119.8(2)	C(3)−N(2)−C(14)	117.6(3)	Cu(1)−N(2)−C(15)	119.6(1)	C(2)−C(1)−C(2)*	124.54(24)
Cu(2)−N(4)−C(24)	122.1(2)	Cu(2)−N(4)−C(27)	121.4(2)	C(3)−N(2)−C(15)	115.9(2)	N(1)−C(2)−C(1)	125.4(2)
C(24)−N(4)−C(27)	116.5(3)	Cu(2)−N(5)−C(25)	123.6(2)	C(2)−C(1)−C(3)	124.3(2)		
Cu(2)−N(5)−C(36)	117.5(2)	C(25)−N(5)−C(36)	118.8(3)	N(1)−C(2)−C(1)	125.6(2)		
C(2)−C(1)−C(3)	124.2(3)	N(1)−C(2)−C(1)	125.6(3)	N(2)−C(3)−C(1)	125.1(2)		
N(2)−C(3)−C(1)	124.6(3)	C(24)−C(23)−C(25)	123.8(3)				
N(4)−C(24)−C(23)	126.2(3)	N(5)−C(25)−C(23)	124.7(3)				

[a] Estimated standard deviations are given in parentheses. Definitions of the least-squares planes follow. For $[Cu^{II}(^{H}L^{Ph})_2]$: plane 1, N(1)−Cu(1)−N(2); plane 2, N(1)*−Cu(1)−N(2)*. For $[Cu^{II}(^{CN}L^{Ph})_2]$: plane 1, N(1)−Cu(1)−N(2)*; plane 2, N(1)*−Cu(1)−N(2). For $[Cu^{II}(^{NO_2}L^{Ph})_2]$: plane 1, N(1)−Cu(1)−N(2); plane 2, N(1)*−Cu(1)−N(2)*. For $[Cu^{II}(^{NO_2}L^{Dtbp})_2]$: plane 1, N(1)−Cu(1)−N(2); plane 2, N(4)−Cu(1)−N(5).

process of $[Cu^{II}(^{Me}L^{Ph})_2]$ and $[Cu^{II}(^{H}L^{Ph})_2]$ indicates that the copper(I) state of the bis(β-diketiminate) complex is unstable with such ligands. Instability of these copper(I) complexes could be attributed to the strong electron-donating nature of $^{Me}L^{Ph-}$ and $^{H}L^{Ph-}$. On the contrary, less electron-donating ligands having the electron-withdrawing substituents, $^{CN}L^{Ph-}$, $^{NO_2}L^{Ph-}$, and $^{NO_2}L^{Dtbp-}$, can support the one-electron reduced species $[Cu^{I}(\beta\text{-diketiminate})_2]^-$, providing reversible redox couples.

The electrochemical behavior of the distorted tetrahedral copper(II) complexes is worth noting in relation to the ubiquitous type 1 copper biological electron transfer sites, which also possess significantly distorted tetrahedral cupric centers.[22] In general, four coordinate copper(II) complexes favor the square planar geometry, while the copper(I) complex is stabilized when it takes a tetrahedral geometry. In fact, the tetrahedral copper complexes supported by a series of 2,9-disubstituted 1,10-phenanthroline derivatives have very positive redox potentials around 0.84−1.03 V versus SCE, 0.36−0.55 V versus Fc/Fc^+ in CH_2Cl_2.[23,24] In the present β-diketiminate ligand systems, the bulky aromatic *N*-substituent also reinforces the copper(II) complexes to exhibit the distorted tetrahedral geometry (Figure 2), which may cause a positive shift of the reduction potential as in the case of the former complexes.[23,24] However, due to the

(22) Randall, D. W.; Gamelin, D. R.; LaCroix, L. B.; Solomon, E. I. *JBIC, J. Biol. Inorg. Chem.* **2000**, *5*, 16−19.
(23) Miller, M. T.; Gantzel, P. K.; Karpishin, T. B. *Inorg. Chem.* **1999**, *38*, 3414−3422.
(24) Connelly, N. G.; Geiger, W. E. *Chem. Rev.* **1996**, *96*, 877−910.

Table 5. Absorption Spectral and ESR Data of the Bis(β-diketiminate) Copper(II) Complexes

	$[Cu^{II}(^{Me}L^{Ph})_2]$	$[Cu^{II}(^{H}L^{Ph})_2]$	$[Cu^{II}(^{CN}L^{Ph})_2]$	$[Cu^{II}(^{NO_2}L^{Ph})_2]$	$[Cu^{II}(^{NO_2}L^{Dtbp})_2]$
			λ_{max},[a] nm (ϵ, M^{-1} cm^{-1})		
	409(14 100)	401(27 900)	389(45 400)	369(46 600)	381(51 800)
	443(16 700)	441(11 900)			
	471(11 600)		496(382)	439(1880)	462(2240)
	571(840)	549(394)	600(145)	590(174)	623(342)
	717(1050)	697(456)	671(1580)	643(1660)	705(1480)
	1566(283)	1422(258)	1328(234)	1200(308)	1305(160)
			ESR[b]		
$g_{\|\|}$	2.182	2.198	2.205	2.210	2.214
$g_{\perp}$	2.054	2.055	2.055	2.055	2.056
$A_{\|\|}$,G	125	126	128	132	129

[a] In THF at 25 °C. In case the absorption bands are overlapped, the λ_{max} and ϵ values were determined by spectral resolution using Gaussian functions with Igor Pro (ver 4, Hulinks). [b] ESR measurements were performed on frozen THF solutions of the copper(II) complexes at −150 °C.

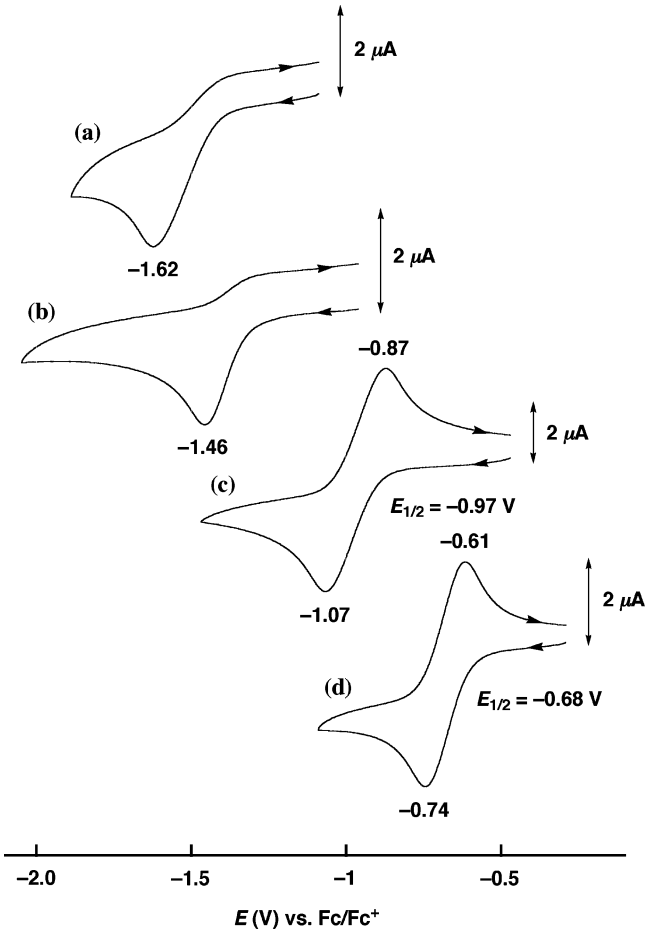

Figure 3. Cyclic voltammograms of (a) $[Cu^{II}(^{Me}L^{Ph})_2]$, (b) $[Cu^{II}(^{H}L^{Ph})_2]$, (c) $[Cu^{II}(^{CN}L^{Ph})_2]$, and (d) $[Cu^{II}(^{NO_2}L^{Ph})_2]$ (1.0×10^{-3} M) in THF containing 0.1 M TBAP; working electrode Pt, counter electrode Pt, pseudoreference electrode Ag, scan rate 0.1 V s^{-1}.

negative charge of the β-diketiminate ligands, the redox potentials of the bis(β-diketiminate) copper(II) complexes are significantly negative even though they possess nearly tetrahedral geometry. Nonetheless, the β-diketiminate ligands with the electron-withdrawing substituents, $^{CN}L^{Ph-}$, $^{NO_2}L^{Ph-}$, and $^{NO_2}L^{Dtbp-}$, can accommodate the copper(I) state, providing the reversible redox couple of copper(II)/copper(I). Thus, these complexes serve as valuable models for investigating the electronic structures of tetrahedral copper(II) complexes, and the results may relate to the active sites of blue copper proteins.

Steric Effects of *ortho*-Substituents of *N*-Aromatic Groups (R^3). In contrast to the former complexes supported by the ligands with R^3 = Ph or Dtbp, the reaction of $^{CN}L^{Mes}H$ or $^{CN}L^{Dep}H$ with $Cu^{II}(OAc)_2$ gave a di(μ-hydroxo)dicopper(II) complex as shown in Figure 4a,b. A similar di(μ-hydroxo)dicopper(II) complex was also obtained, when $^{NO_2}L^{Mes}H$ was treated with $Cu^{II}(OAc)_2$ under the same experimental conditions. The crystal structure of the di(μ-hydroxo)dicopper(II) complex supported by $^{NO_2}L^{Mes-}$ was reported in the previous paper.[3e] In these cases, each copper ion exhibits a square planar geometry consisting of a N_2O_2 donor set, which is provided from the didentate ligands and the bridging OH groups. All the di(μ-hydroxo)dicopper(II) complexes were ESR silent due to a strong magnetic interaction between the two cupric ions through the μ-hydroxo bridges. Since the Cu−O−Cu angle of the complex is 102−105° (see Table 4), the magnetic interaction may be antiferromagnetic. Crawford and co-workers have established the linear correlation between the Cu−O−Cu angle (θ) of a series of di(μ-hydroxo)dicopper(II) complexes and their singlet−triplet exchange parameter J as $2J = -74.53\theta + 7270$ cm^{-1}.[25] From this correlation, it was concluded that when θ is larger than 97.55°, the overall magnetic behavior is antiferromagnetic. Such a large Cu−O−Cu angle in the di(μ-hydroxo)dicopper(II) complexes supported by the β-diketiminate ligands may be due to the steric repulsion between the *N*-aromatic groups. The complexes $[Cu^{II}_2(^{CN}L^{Mes})_2(\mu\text{-}OH)_2]$ and $[Cu^{II}_2(^{CN}L^{Dep})_2(\mu\text{-}OH)_2]$ also exhibit a strong ligand based $\pi-\pi^*$ band at 345 nm (ϵ = 33 100 M^{-1} cm^{-1}) and 340 (32 900), respectively, together with an LMCT band at ∼440 (3900) and n−π^* at ∼540 (300−500). The d−d bands of these complexes ∼800 nm are significantly weak and broadened. The di(μ-hydroxo)dicopper(II) complexes gave two irreversible reduction peaks at siginificantly negative positions: −2.10 and −2.85 V versus Fc/Fc^+ for $[Cu^{II}_2(^{CN}L^{Mes})_2(\mu\text{-}OH)_2]$ and −2.05 and −2.81 V versus Fc/Fc^+ for $[Cu^{II}_2(^{CN}L^{Dep})_2(\mu\text{-}OH)_2]$. The irreversibility in the electrochemical measurements clearly indicates that the reduction of the dinuclear copper(II) complex induces degradation of the di(μ-hydroxo)dicopper core.

The steric effect of the *ortho*-substituents of R^3 is more prominent in the case of $^{CN}L^{Dipp}H$. In this case, the mono-

(25) Crawford, V. H.; Richardson, H. W.; Wasson, J. R.; Hodgson, D. J.; Hatfield, W. E. *Inorg. Chem.* **1976**, *15*, 2107−2110.

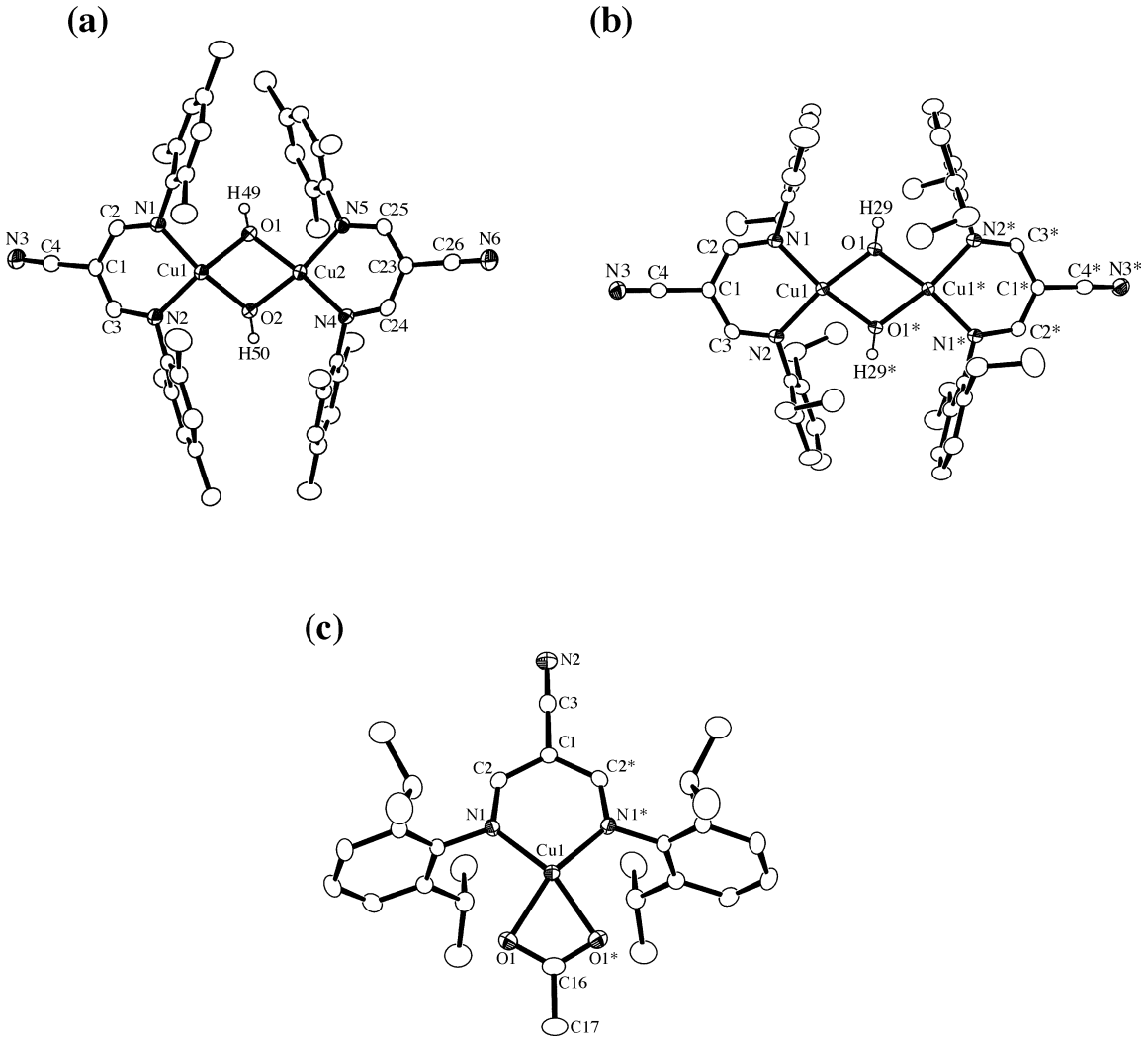

Figure 4. ORTEP drawings of (a) $[Cu^{II}_2(^{CN}L^{Mes})_2(\mu\text{-}OH)_2]$, (b) $[Cu^{II}_2(^{CN}L^{Dep})_2(\mu\text{-}OH)_2]$, and (c) $[Cu^{II}(^{CN}L^{Dipp})(AcO)]$ with 50% probability thermal ellipsoids. Hydrogen atoms except the one at the hydroxy group [H(49) and H(50) of a, H(29) and H(29)* of b] are omitted for clarity.

nuclear copper(II) complex supported one β-diketiminate ligand $^{CN}L^{Dipp-}$ and one didentate acetate ion as shown in Figure 4c. The cupric ion exhibits a distorted square planar geometry showing an ESR spectrum with $g_{\|} = 2.257$, $g_{\perp} = 2.057$, and $A_{\|} = 172$ G. The UV−vis spectrum of this complex is similar to that of the di(μ-hydroxo)dicopper(II) complexes [344 nm ($\epsilon = 20200\ M^{-1}\ cm^{-1}$), 440 (754), 580 (150), ∼700 (120)], and the compound gave an irreversible reduction peak at −1.17 V vs Fc/Fc^+ in THF.

In summary, mononuclear and dinuclear copper(II) complexes supported by a series of β-diketiminate ligands have been synthesized, and their structures and physicochemical properties have been investigated systematically. The metal centers of these complexes are all enforced to have four-coordinate structures, but their coordination geometries are significantly altered, providing the distorted tetrahedral copper(II), planar di(μ-hydroxo)dicopper(II), and distorted square planar copper(II) complexes, depending on the *N*-aromatic substituents of the β-diketiminate ligands. The copper(II) complexes supported by $^{Me}L^{Ph-}$, $^{H}L^{Ph-}$, $^{CN}L^{Ph-}$, $^{NO_2}L^{Ph-}$, and $^{NO_2}L^{Dtbp-}$ possess essentially the same distorted tetrahedral structure, but different spectroscopic and electrochemical features. Thus, these complexes provide an excellent opportunity to examine the electronic effects of the ligands on the redox functions of the distorted tetrahedral copper(II) complexes. Chemical functions of the mononuclear and dinuclear copper(II) complexes are now under investigation.[26]

Acknowledgment. The authors thank Professor H. Nakazawa of Osaka City University for his valuable comments and discussions. This work was financially supported in part by Grants-in-Aid for Scientific Research on Priority Area (11228206) and Grants-in-Aid for Scientific Research (13480189) from the Ministry of Education, Culture, Sports, Science and Technology, Japan.

Supporting Information Available: X-ray structural determination and details of the crystallographic data as a CIF file. This material is available free of charge via the Internet at http://pubs.acs.org.

IC0344766

(26) A preliminary study on the reaction of H_2O_2 and the mononuclear copper(II)−acetate complex supported by $^{CN}L^{Dipp-}$ has suggested formation of a thermally stable copper(II)−peroxo complex that is a subject of a separate report.